Int. J Multiphase Flow Vol 11, No. 5, pp 659–674, 1985
Printed in Great Britain.

0301-9322/85 $3.00 + .00
Pergamon/Elsevier

AN EXPERIMENTAL INVESTIGATION OF GAS–PARTICLE FLOWS THROUGH DIFFUSERS IN THE FREEBOARD REGION OF FLUIDIZED BEDS

SUNIL R. KALE and JOHN K. EATON
Thermosciences Division, Department of Mechanical Engineering, Stanford University, Stanford, CA 94305, U.S.A.

(*Received* 1 *August* 1984; *in revised form* 30 *January* 1985)

Abstract—The phenomenon of particulate loss (elutriation) from fluidized beds is important in many industrial processes. Results reported in Kale & Eaton (1984a) showed that very-wide-angle diffusers located in the freeboard above a fluidized bed substantially reduce elutriation—a result that was contrary to intuition. The present experiment was designed to explain these results. The same fluidized bed apparatus (Kale & Eaton 1984a) was used—150 mm square in cross section with a variable-angle diffuser in the freeboard region. Glass beads (nominally 50–100 μm in diameter) were fluidized by air at atmospheric pressure in the bubbling regime. Gas-phase velocity measurements were made using a single-component laser–Doppler anemometer. Four diffuser configurations (0, 20, 40 and 60° full opening angle) were studied. One set of measurements was made with the bed in place and a second set with the bed material removed. The flow structure was drastically altered by the presence of the fluidized bed below the diffuser. The single-phase flow was separated in the diffuser for the 20, 40 and 60° cases. However, the flow did not separate in the presence of the bed, and the peak fluid velocities were lower than those in the separated flow. This behavior is responsible for the decrease in the elutriation rate with increasing diffuser opening angle. A simple analysis suggests that suspended particles in the diffuser flow are responsible for the change in the flow structure. Momentum loss from the gas to the suspended particles reduces the pressure gradient, thereby eliminating the tendency to separate.

1. INTRODUCTION

Since their invention, fluidized beds have found extensive applications in industry. Processes involving fluidized beds are found today in almost all the major industries—coal, combustion, petroleum-cracking units, mineral processing, metallurgical processes, heat exchangers, food processing, etc. Many of the industrial fluidized beds operate in the bubbling regime because of its unique characteristics, the most notable being very uniform properties due to thorough mixing. The bubble motion through the bed causes not only local mixing but also large-scale circulation within the bed. The diverse applications of the fluidized bed have thrown up a host of problem areas closely associated with bubbling. One of the consequences of bubbling is the elutriation (carryover) of particles from the bed due to bubble passage through the bed surface.

For the industrial applications cited earlier, it is important to limit the loss of process particles, i.e. minimize elutriation. Changing bed operating parameters or modifying the bed geometry is possible, but not without economic penalty. External cleanup devices such as cyclone separators, electrostatic precipitators and baghouse filters are frequently used for particulate cleanup. The effects of bed geometry on elutriation have not been extensively studied as a possible control technique.

It is not uncommon for designers to incorporate diffusing sections in the freeboard region of fluidized bed reactors. Apart from accommodating cyclones, these diffusing sections ostensibly serve the purpose of reducing elutriation from the reactors. This design practice is lent credence by the one-phase flow observations on diffusers. In general, optimum pressure recovery and fluid deceleration are obtained for diffuser full openings of ~12–18°. It would therefore be expected that such a diffuser would be most effective in disengaging particles, thus reducing elutriation as a result of slower-moving fluid. However, industrial diffusers similar to those in catalytic cracking units typically have diffuser openings in the range of 70–80°.

On the basis of one-phase flow observations, it appears doubtful that large-angle diffusers would have any effect in reducing the elutriation rate. The flow in this case would be in the jet-flow regime, with little or no flow deceleration and consequently a minimal reduction in the elutriation rate. Elutriation-rate measurements reported earlier (Kale & Eaton 1984a) contradict these predictions. The elutriation rate was found to decrease monotonically with diffuser opening angle up to total included angles of 60°. Figure 1 illustrates this behavior for a range of gas velocities and a configuration in which the diffuser inlet is well downstream of the bed surface.

The objective of the present study was to explain the results shown in figure 1. Profiles of the gas-phase velocity were measured in the diffuser both in the presence of the fluidized bed and with the bed particles removed. Laser–Doppler anemometry (LDA) was used because it is particularly well suited for measurements in particle-laden flows.

The uniqueness of the present research program is highlighted by the fact that virtually no literature exists on the specific problem being addressed—effects of diffusers on elutriation rates from fluidized beds. There are large bodies of literature in several related areas, including fluidized bed phenomena, turbulent particulate flows, diffuser flows and diagnostic techniques for particulate flows. The literature in each of these related areas is reviewed in Kale & Eaton (1984b).

One previous experiment by Levy & Lockwood (1983) was of particular relevance to the present work. They used an LDA to measure gas-phase velocities above a bed in which 400- to 1000-μm sand was fluidized. Their channel was rectangular in cross section and larger (305 × 610 mm) than the present facility. Their results are compared with the present results in the discussion section.

2. EXPERIMENTAL EQUIPMENT AND PROCEDURES

2.1 *The fluidized bed*

Figure 2 illustrates the important features of the fluidized bed. The lower half of the apparatus, 150 mm square section and 1015 mm high, is a straight section that incorporates three major components of the fluidized bed—windbox and distributor, dense bed region and the freeboard region prior to the diffuser. The entire section is made of Plexiglas and glued at the edges to form a leakproof channel. The distributor is 3-mm-thick, sintered bronze with openings in the range of 25–50 μm. This prevents the particles from falling through, at the same time providing uniform air distribution across the entire surface during bed operation. The remaining 915 mm above the distributor plate can be utilized as the dense portion of the fluidized bed, where 50- to 100-μm glass beads were fluidized with atmospheric air.

The upper half of the bed is flexible to incorporate a variable-angle diffuser. This section has a uniform depth of 150 mm, but the sidewalls may be angled to form a straight-walled diffuser with an opening angle ranging from 0 to 60°. Flexible joints at points A and B provide a smooth transition from the straight to the angled walls. It should be noted that the diffuser flow is not two dimensional. The inlet is square, and when the diffuser angle is opened up, the exit aspect ratio (depth/width) is much less than unity.

All the experiments on the fluidized bed were performed with material comprised of glass beads with diameters ranging from 20 to 100 μm, with the bulk of the particles in the range of 50–100 μm. A sieve analysis of the particles is given in table 1. Observations under a microscope indicated that the glass beads were spherical in shape.

Air flow for fluidization was taken from a compressed air reservoir through regulating and gate values that provided stable air flow in the system during the bubbling process. Additionally, flow fluctuations through the bed, caused by bubble bursts, were damped out by introducing extra flow resistance in the form of steel-wool plugs in the pipe near the inlet to the windbox. A set of filters and dryers served to clean the air entering the bed.

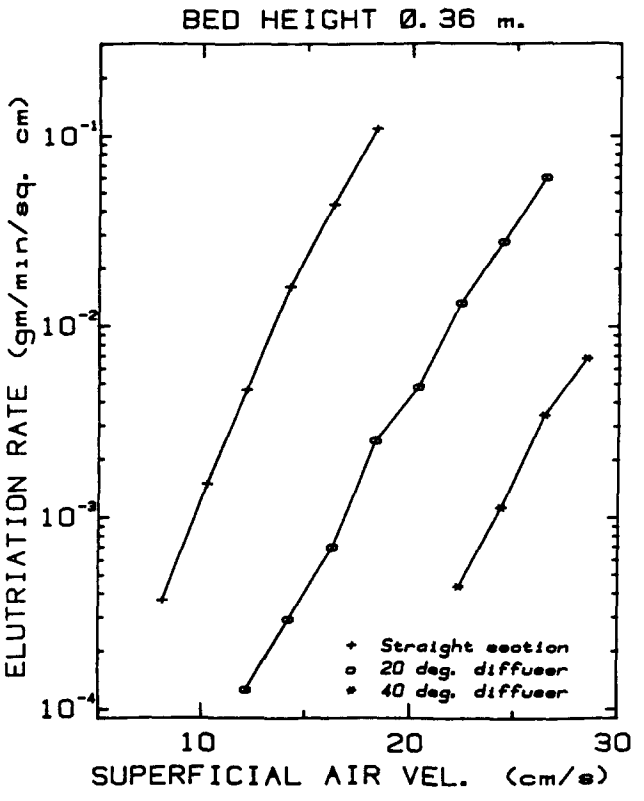

Figure 1. Effect of superficial air velocity on elutriation rates (bed height = 0.36 m).

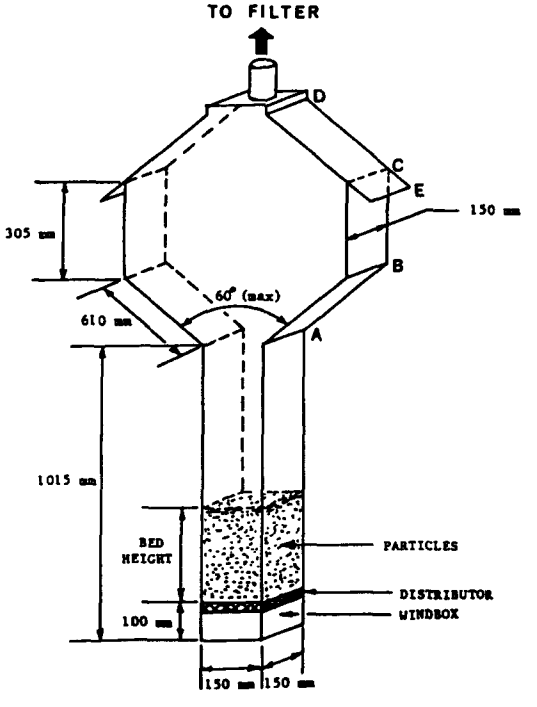

Figure 2. Major dimensions of the fluidized bed apparatus.

Table 1. Sieve analysis of bed particles

Sieve size (μm)	Weight of % retained
106	0.6
75	46.9
63	16.8
53	17.7
45	15.7
<45	2.3

2.2 *LDA*

Pointwise velocity measurements above the bed were made possible by a single-component LDA system. The light source was a 5 mW helium–neon laser (wavelength 632.8 nm), and the system was arranged in the forward-scatter mode. The entire optics were mounted on a U-shaped horizontal traverse base, which in turn was mounted on a vertical traverse base. The combination of the two traverse mechanisms allows scanning of the entire diffuser at maximum opening angle. Motion and simultaneous alignment were enabled by two sets of linear bearings, one set for each traverse. Positioning of the traverse was done manually.

The traverse and the optics were designed to focus the laser beams on the centerplane between the two face plates. Details of this arrangement are shown in figure 3. The transmitting optics consists of a beam splitter, a Bragg cell for frequency shifting one beam and the focusing lens.

The system was set up to measure the vertical component of the gas-phase velocity. The 50- to 100-μm particles thrown up from the bed surface are too large to follow the gas flow, so 1-μm alumina was used to seed the flow. Alumina powder was added to the bed through a side port prior to each run and then at regular intervals. During bed operation, this alumina was mixed with the bed, thus breaking up agglomerates. The bubble flow through the bed carries away these particles, thus seeding the freeboard flow. Doppler signals were obtained from both bed particles and seeding particles, so it was necessary to eliminate signals from

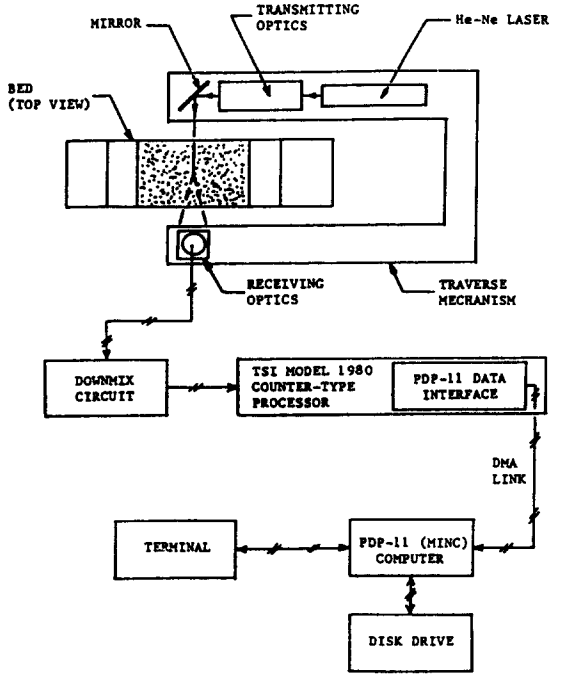

Figure 3. Schematic of the LDA and data-acquisition systems.

the former to obtain the gas-phase velocity. The large-particle Doppler bursts exhibited a very large pedestal and were eliminated using an amplitude discriminator on the signal processor. The concentration of seed particles was much higher than that of bed particles; consequently, only a small fraction of the Doppler bursts were spurious.

In the bed-removed case (one-phase flow), oil smoke was used as the seed material. The oil droplets were produced by a TEM Model NPL-type smoke generator, in which mineral oil is passed over a heated element to produce oil vapor/smoke. This smoke generator was positioned at the bottom of the windbox through a port.

The signal-processing hardware consisted of a counter-type processor (TSI Model 1980) and a laboratory computer, as shown in figure 3. The data were transferred from the processor to the computer via a direct-memory access interface. The data rate was monitored on a TSI Model 1992 Readout Unit and the Doppler signals continuously observed on a Tektronix digital oscilloscope.

2.3 *Experimental procedures*

Two sets of data were obtained, one without the bed (clean one-phase flow) and one with the bed. For each set, four geometries were studied: 0 (straight section), 20, 40, and 60° full diffuser openings. A bed height of 0.36 m and a superficial air velocity of 0.14 m/s were selected, resulting in a bubbling bed. The relatively shallow bed and low speed avoided dense sprays of large particles in the diffuser, while still exhibiting the common behavior of decreasing elutriation rate with increasing diffuser angle (Eaton & Kale 1984a).

Mean velocity and turbulence intensity profiles were measured at two axial locations—one halfway through the diffuser (location 1) and the other just before the diffuser exit (location 2). Profiles closer to the diffuser inlet were unobtainable because of particles coating the face plates.

Periodic sampling of the digital output from the LDA processor was used to eliminate velocity bias that would result from simple particle averaging (McLaughlin & Tiederman 1973). Stevenson & Thompson (1982) and Adams *et al.* (1984) have shown that velocity bias is negligible if periodic sampling is used and the particle arrival rate is high. The validated particle arrival rate was between 100 and 200 Hz, except near the wall where it was reduced to 50–70 Hz. A periodic sampling rate of 25 Hz was used except near the wall, where it was reduced to 15 Hz. Characteristic frequencies in the flow were of the order of 1 Hz.

Running averages of the mean velocity and turbulence intensity were computed and sampling continued until reasonable convergence was obtained. Sampling periods of 3–7 min were required, owing to the low frequencies dominant in the flow.

Based on the method of uncertainty calculation as given by Kline & McClintock (1953), uncertainties in the fringe spacing are estimated at 0.5%, corresponding to a similar uncertainty in the velocity measurement. In addition, uncertainties in the velocity measurements would show up owing primarily to repeatability of a measurement. When measuring velocities in a flow with very-low-frequency unsteadiness, e.g. in a separating diffuser, the uncertainties are estimated to be as high as 25% in some cases. For the cases presented here, the uncertainties are estimated at $<10\%$ for clean one-phase flow. When measuring gas-phase velocities with the bed material in place, the velocity measurements were observed to be repeatable within 5% of the value, at most, and lower, ~3%, in most cases. The uncertainties in the root mean square (r.m.s.) velocities are estimated at ~10%.

3. EXPERIMENTAL RESULTS

Axial mean velocity and turbulence intensity profiles are presented in unnormalized form in this section. The coordinate normal to the flow is designated y and has its origin on the centerline of the channel. The width of the flow channel varies, so the location of the wall

is indicated on each plot. The vertical coordinate (z) of the two measurement stations varies, because the diffuser gets shorter as the opening angle decreases. The actual value of z measured from the distributor is given on each plot.

Figures 4 and 5 show the mean velocity profiles at two consecutive z-locations for the straight section. In the absence of the bed, the profiles resemble those of a developing flow in a square channel. The low Reynolds number of the flow accounts for the thick boundary layers. The mean velocity profiles in the presence of the bed show remarkably uniform features and very little change between location 1 and location 2. Since the mean velocity is uniform, it must be equal to the superficial air velocity defined as the volume flow rate of air divided by the cross-sectional area. This fact provided an independent check of the validity of the velocity data, since the volume flow rate into the bed was measured using a rotameter. The velocities measured using the LDA agreed with the known superficial air velocity to within the experimental uncertainty.

The turbulence intensities for these cases are shown in figures 6 and 7 for the same consecutive z-locations. Increasing turbulence intensities closer to the walls are the norms for the profile without the bed, indicating the growth of wall boundary layers. Against the above, the turbulence intensities in the presence of the bed are significantly higher and at the same time fairly uniform across the bed cross section. Further, the streamwise distance does not have any significant effect on the nature of the turbulence profile. The large turbulence intensity in the presence of the bed is caused by bubbles bursting at the surface of the bed. The unsteadiness apparently decays quite slowly at this distance above the bed's surface.

The mean velocity profiles are substantially different for the 20° diffuser, as shown in figures 8 and 9. In the absence of the bed, separation is observed to occur on one wall of the diffuser. This separation was observed to occur preferentially on one wall of the diffuser, and no switchings were observed during a run. Further, the mean velocity profiles show a distinct development of the recirculating region, confirming the diffuser flow to be in the fully stalled mode. A striking conclusion that emerges from the profiles in the presence of the bed is that there is no backflow at either location. The profiles exhibit remarkable uniformity across the span, and a fall in the peak velocity corresponding to the area expansion at each z-location is evident.

The trend in the turbulence intensities is shown in figures 10 and 11. A significant increase in the turbulence intensities is seen at the separation region, indicating growth of the shear layer in the case of a clean flow. A smaller peak on the left side of the diffuser shows the boundary-layer growth.

In the presence of the bed, there are significant changes to the r.m.s. velocity profiles. As against sharp variations in the turbulence levels for the single-phase flow case, the bed flow exhibits a smaller range. Furthermore, these turbulence level variations of 40–60% at location 1 and 30–50% at location 2 are of the same order as that in the straight-channel case. The two figures also indicate a decrease of ~30–40% in turbulence intensity between $z = 130$ cm and $z = 150$ cm.

The single-phase 40° diffuser exhibits two modes—a fully stalled mode similar to the 20° diffuser and a jet-flow mode. Neither mode is stable, and the flow switches occasionally from one to the other. Profiles for this case are not shown, because the low-frequency mode switching causes excessive scatter. The particulate flow above the bed remains fully attached.

Mean velocity profiles for the 60° diffuser are shown in figures 12 and 13. In the absence of a bed, the 60° diffuser operated consistently in the jet-flow mode, as the velocity profiles clearly show. The growth of the recirculating region is distinctly observable in these diagrams. Only a slight decay in the peak velocity is observed with increasing z-locations.

In the presence of the bed, the absence of any separation is again evident in the case of the 60° diffuser. However, this geometry does not exhibit the uniform velocity that other

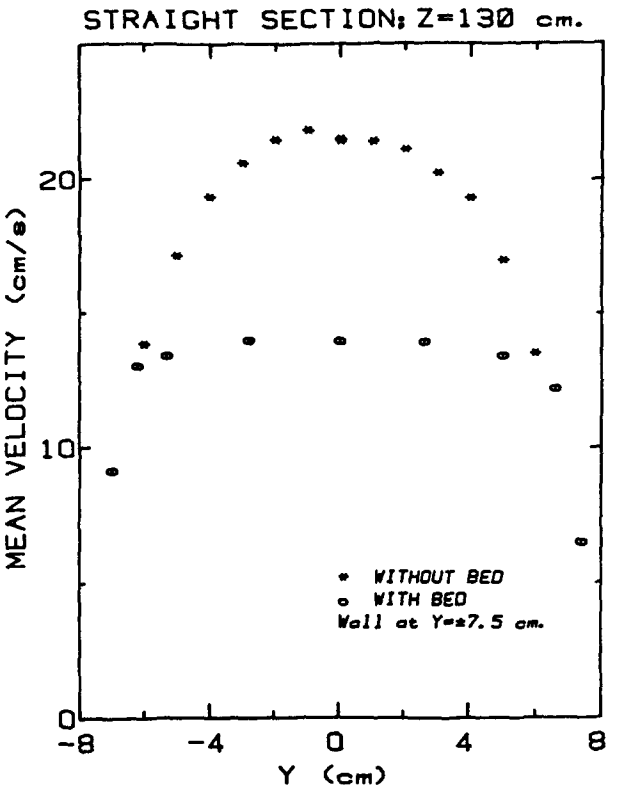

Figure 4. Mean velocity profiles for straight section at location 1 (z = 130 cm).

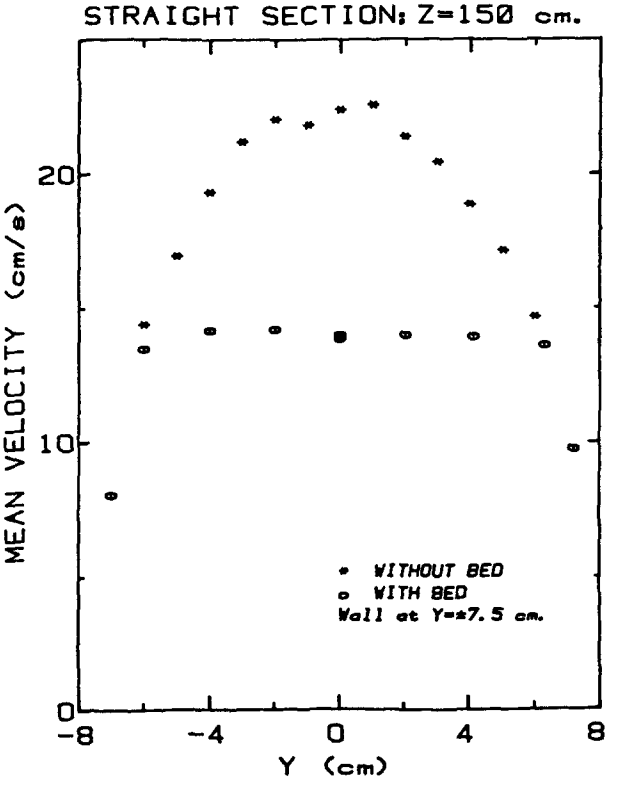

Figure 5. Mean velocity profiles for straight section at location 2 (z = 150 cm).

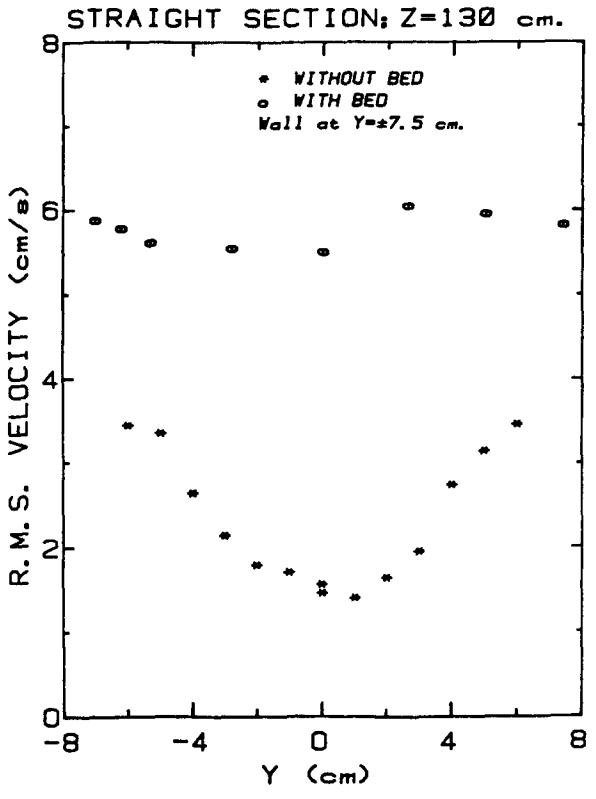

Figure 6. Turbulence profiles for straight section at location 1 (z = 130 cm).

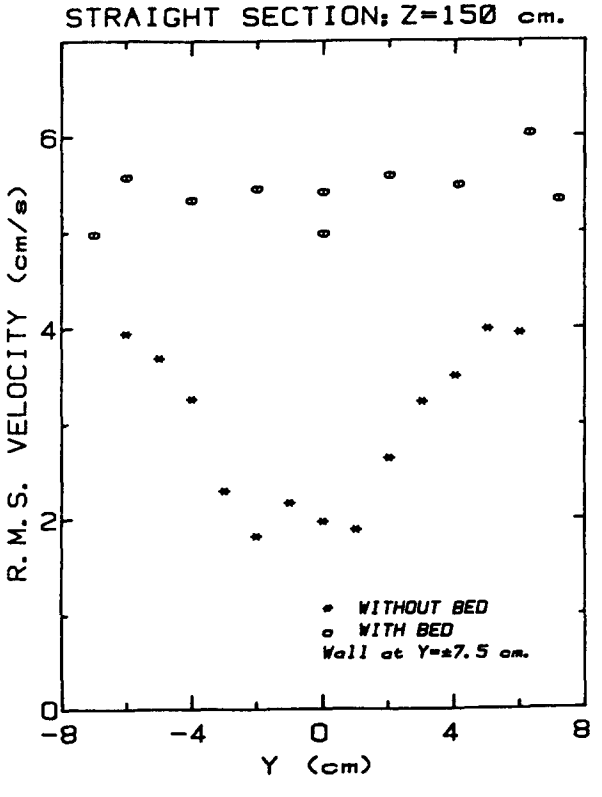

Figure 7. Turbulence profiles for straight section at location 2 (z = 150 cm).

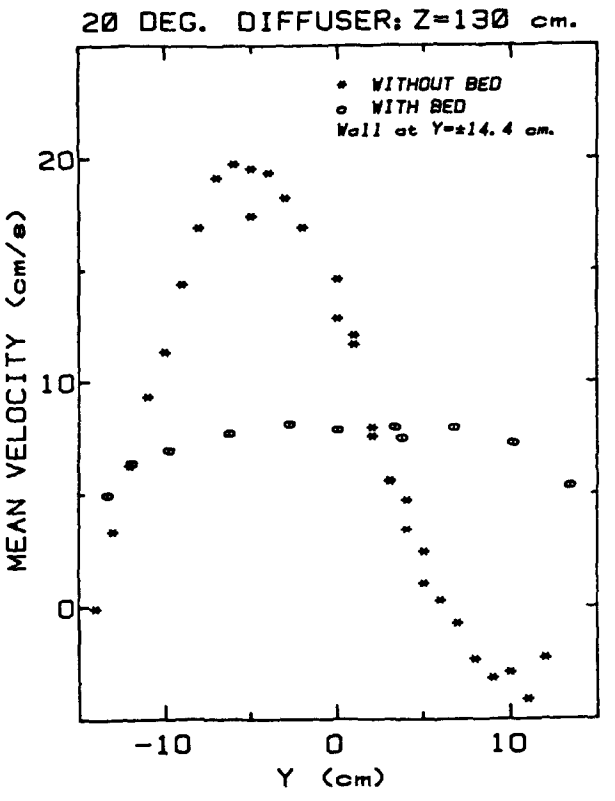

Figure 8. Mean velocity profiles for 20° diffuser at location 1 (z = 130 cm).

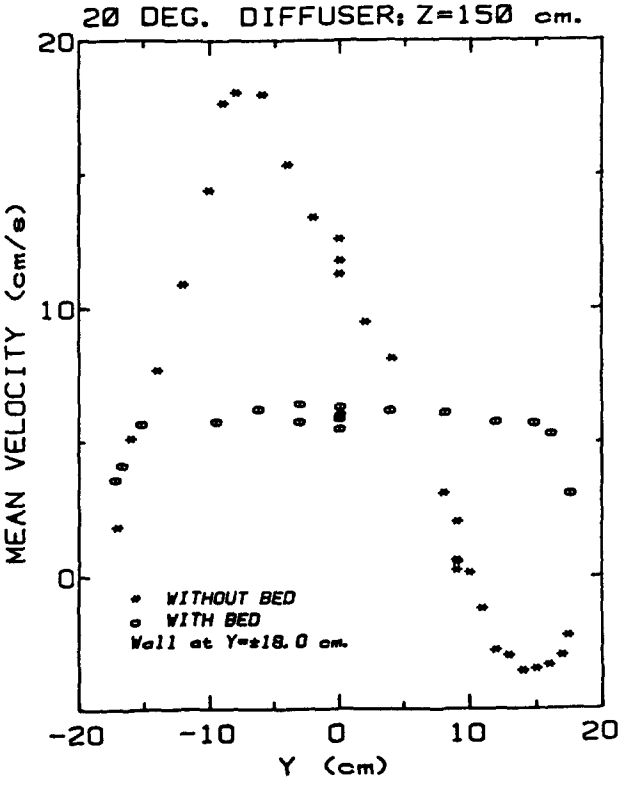

Figure 9. Mean velocity profiles for 20° diffuser at location 2 (z = 150 cm).

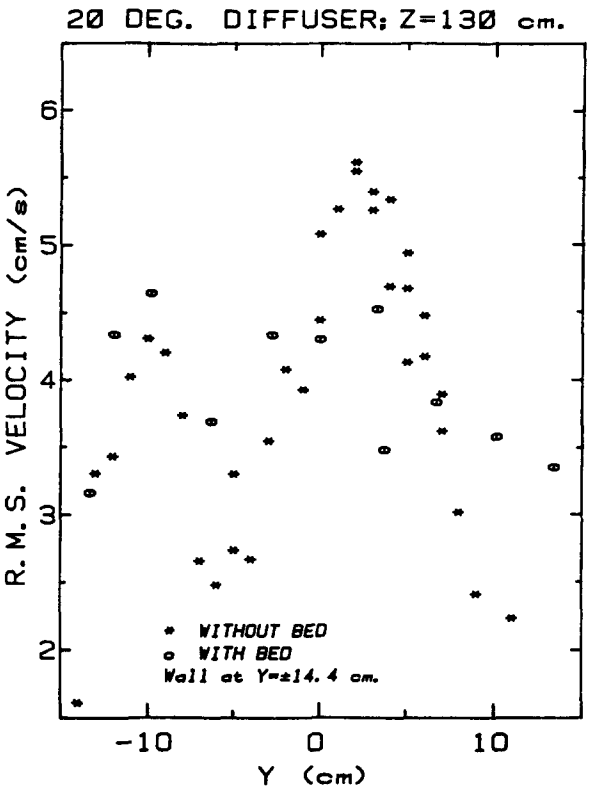

Figure 10. Turbulence profiles for 20° diffuser at location 1 (z = 130 cm).

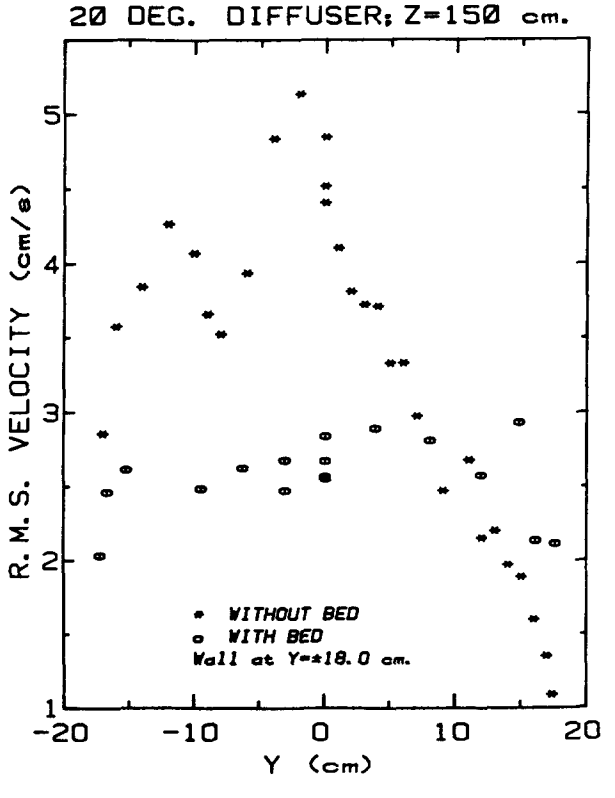

Figure 11. Turbulence profiles for 20° diffuser at location 2 (z = 150 cm).

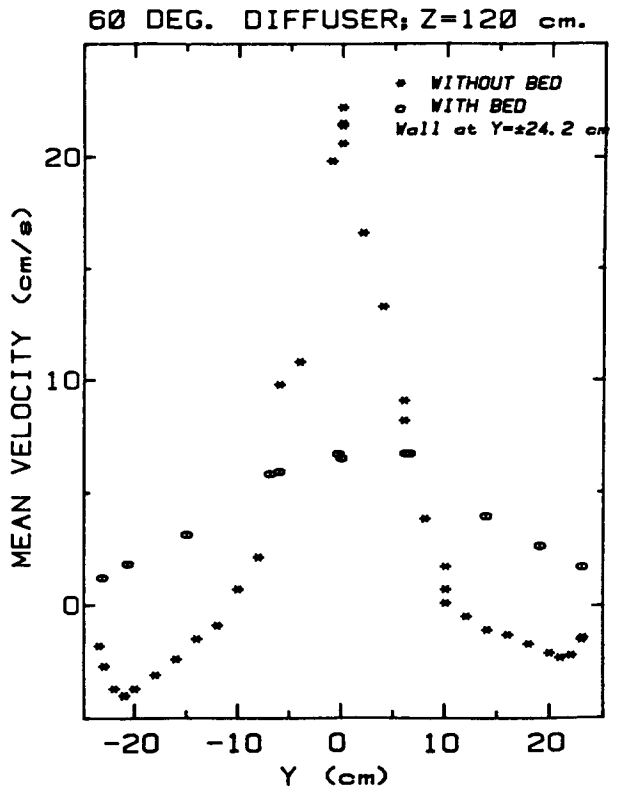

Figure 12. Mean velocity profiles for 60° diffuser at location 1 (z = 120 cm).

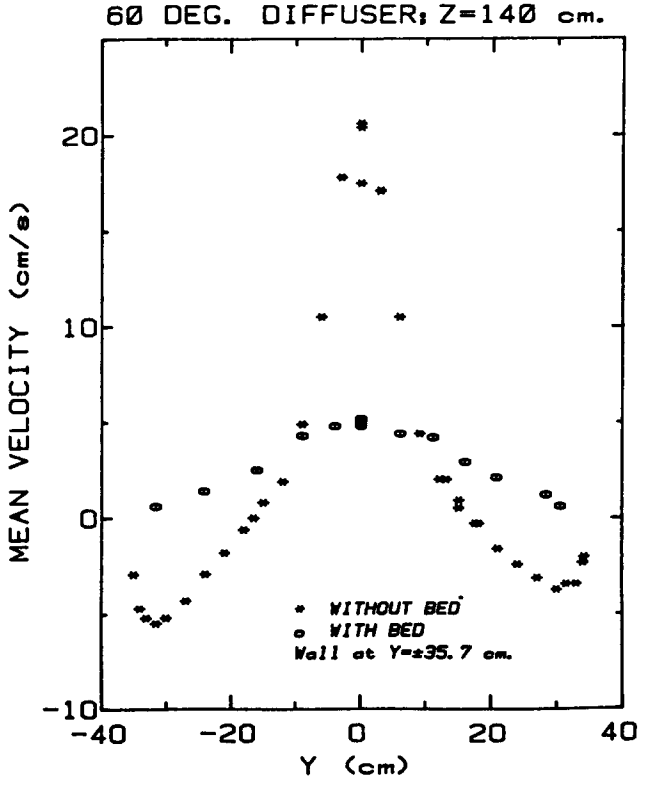

Figure 13. Mean velocity profiles for 60° diffuser at location 2 (z = 140 cm).

geometries exhibited. Instead, the mean velocity profiles resemble a jet flow. The peak velocities, however, are significantly lower than corresponding values for the clean one-phase flow.

The turbulence profiles for the 60° diffuser are shown in figures 14 and 15. The shear layers can be seen to come closer and almost merge. As this flow develops on its way through the diffuser, the wall boundary-layer growth in the recirculating regions is clearly marked by a small peak close to each wall. In the presence of the bed, the turbulence level was fairly uniform and decayed in the streamwise direction, as in the previous two configurations.

4. DISCUSSION

Velocity profiles with the straight section indicate that the clean, one-phase flow grows as a developing channel flow, marked by growing boundary layers and an increase in the core velocity. On the other hand, profiles above the bubbling bed indicate an almost uniform velocity across the bed cross section. There is very little boundary-layer growth as the flow moves up the passage, and the boundary-layer blockage is negligible. The lack of boundary-layer growth can be attributed to a strongly favorable pressure gradient in the freeboard region, as will be discussed below. Although the boundary layers were thin, the velocity profiles decreased monotonically toward the wall. No secondary peaks were observed.

The uniform flow above the bed indicates that the distributor was quite uniform and that the bed flow was not dominated by large bubbles. Excessively large bubbles or slugging would create a nonuniform mean flow, with a peak velocity expected near the channel center.

The present results were in sharp contrast to the measurements of Levy & Lockwood (1983), who found nonmonotonic variations in the velocity. They observed peak velocities occurring near the wall rather than in the channel center for U/U_{mf} between 1.3 and 3.0. The reasons for the differences are not clear. Levy & Lockwood propose that the peak velocities near the walls are caused by near-wall bubble bursts. However, it is well documented that bubbles generally coalesce and move toward the bed center as they travel upward. Therefore, the peak velocities occurring near the wall may be a unique feature of Levy & Lockwood's experiment. One possible cause is the rectangular shape of their bed, which had an aspect ratio of 2.

The turbulence intensities measured above the bed for the straight-channel case are fairly uniform and decrease slowly in the axial direction. The turbulent fluctuations are caused by the bubbling process. Near the bed surface, the velocity fluctuations are very large but decay rapidly moving up in the bed. The decay of the largest velocity fluctuations allows the disengagement of large particles from the gas flow. Since the turbulence intensity is decreasing, disengagement is probably still taking place in the present measurement region. However, most of the disengagement occurred lower in the freeboard, where the largest particles fell back to the bed. The decay in the turbulence levels with very little change in the mean velocity profile was also observed by Levy & Lockwood (1983).

The single-phase diffusers all exhibited separation. The 20° diffuser separated on one wall and was fully stalled. The 60° diffuser separated from both walls in a jet flow, whereas the 40° diffuser switched between the fully stalled and jet-flow modes. These observations are in general agreement with the correlations of Fox & Kline (1962).

None of the diffusers exhibited any tendency to separate in the presence of the fluidized bed. Several factors attributable to the bed, individually or in combination, could be responsible for this fact. Particle loading could eliminate the tendency to separate by reducing or eliminating entirely the adverse pressure gradient in the diffuser. Alternatively, inlet turbulence or overall flow unsteadiness could delay separation. Although no information exists on the former (particulate effects), some data are available on the effects of turbulence, unsteadiness and nonuniformities on diffuser fluid mechanics.

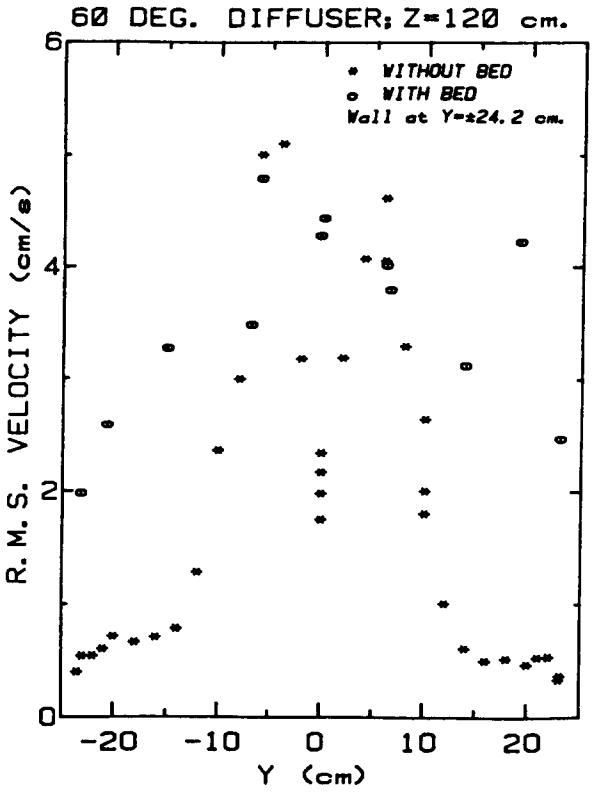

Figure 14. Turbulence profiles for 60° diffuser at location 1 (z = 120 cm).

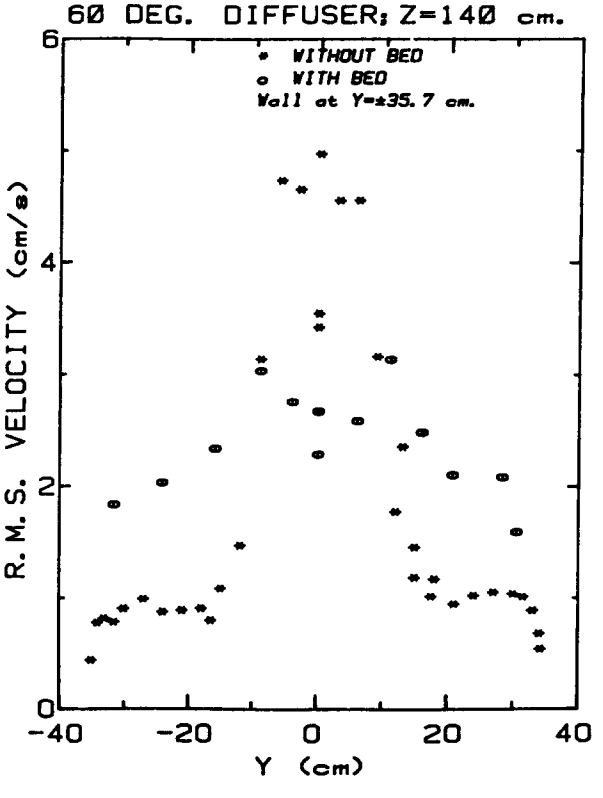

Figure 15. Turbulence profiles for 60° diffuser at location 2 (z = 140 cm).

Cutler & Johnston (1981) have summarized the effects of inlet mean flow nonuniformity and turbulence distributions on diffuser performance. It has been found that mean flow nonuniformity leads to earlier separation and a degradation of diffuser performance. Increased turbulence can enhance boundary-layer mixing and delay separation (Hoffmann 1981). However, even very large turbulence levels would not be enough to force a 60° diffuser to stay attached. Jayaraman (1982) has shown that low-frequency unsteadiness can delay separation in adverse pressure-gradient flows. In a separate experiment (Kale & Eaton 1984b), the authors have shown that large-scale unsteadiness in the absence of particulate loading does not significantly delay separation in the present apparatus.

From the foregoing discussion, it is clear that the inlet nonuniformities and unsteadiness cannot be construed as sufficient conditions for keeping the diffuser flow attached. Particle loading in the diffuser must cause the flow to remain attached by reducing the adverse pressure gradient imposed in a single-phase flow. Bed fines have terminal velocities that range from ~3 cm/s for the smallest particles up to 16 cm/s for 50-μm particles. As the flow decelerates in the expanding passage, the larger fines reach a point where they can no longer move up with the flow and remain suspended until they diffuse to the passage wall. The presence of these particles was detected when they passed slowly through the laser beams and also when they accumulated on the diffuser walls. The suspended particles exert a drag on the gas, which reduces the adverse pressure gradient in the diffuser or even causes a favorable pressure gradient.

The effect of suspended particles described qualitatively above cannot be quantified without measurements of the weight of suspended particles. Such measurements are not available in the present apparatus. However, the mean velocity profiles measured in the straight section with the bed suggest that the flow experiences a strongly favorable pressure gradient. The single-phase flow experiences a slightly favorable pressure gradient, yet thick boundary layers still develop. However, in the flow above the bed, the boundary layers remain very thin. Similar observations can be made in the 20° diffuser flow. Figure 16 shows normalized velocity profiles for the straight section without the bed and for the 20° diffuser with the bed—both at the same z-location, $z = 130$ cm. The spanwise coordinate has been normalized on the diffuser half-width at the corresponding z-location and the streamwise velocity on the maximum measured velocity. The profiles suggest that the presence of the particles in the diffuser flow results in a more favorable pressure gradient, as manifested in thin boundary layers. However, this conclusion cannot be compared with experimental values, because extremely small dynamic heads, calculated as 0.01 Pa for a velocity of 0.14 m/s, prevailing in the diffuser made pressure measurements impossible.

Given this phenomenon of attached diffusers, some interesting facts emerge from the mean velocity profiles. The 20° diffuser exhibits an almost uniform velocity across the entire diffuser cross section; the 40° diffuser exhibits jetlike tendencies in the center of the diffuser; and the 60° diffuser results in an almost jetlike profile. It is thus likely that for openings beyond 60°, the diffuser flow may become a gas–solid jet flow, complete with recirculating regions.

A major link can be provided between these velocity profiles and the elutriation measurements. As the mean velocity profiles indicate, successively larger diffuser openings result in decreasing air velocities. Naturally, then, this would reflect in fewer particles being elutriated, only very small ones being able to flow through. This is expected from Stokes' relations, which show a strong dependence of particle terminal velocity on particle size. Therefore, one would expect a monotonic decrease in elutriation rates with increasing diffuser openings. This fully explains the observed monotonic decrease in elutriation rate for the 0.36-m-high bed.

The experimental results of Kale & Eaton (1984a) showed that all the parameters varied—gas velocity, bed height and diffuser angle—had a significant effect on the

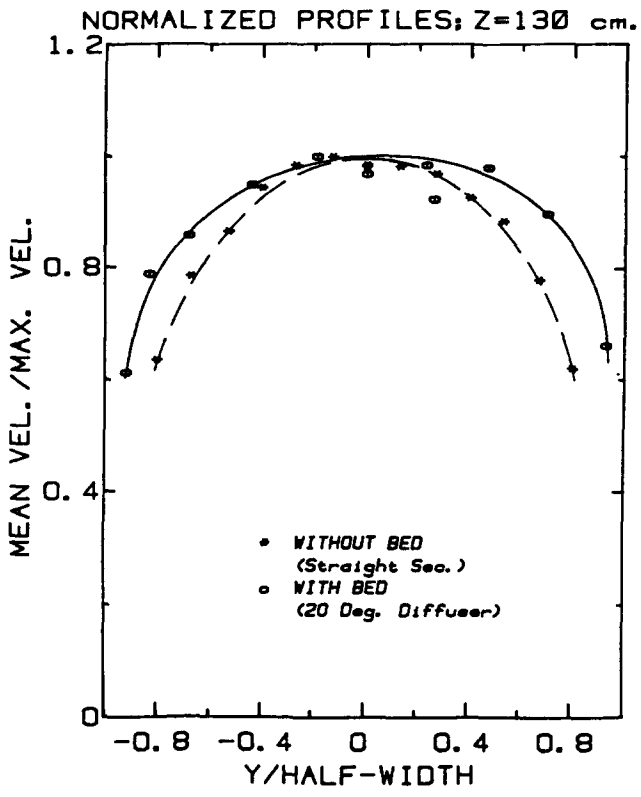

Figure 16. Normalized velocity profiles for z = 130 cm for straight section without bed and for 20° diffuser with bed.

elutriation rate. The elutriation rate increased exponentially with increasing air velocities. Heretofore, this result has been known to be true for straight-section beds. However, the present studies showed that this observation is valid for all diffuser geometries. Further, this conclusion was found to be independent of the bed height.

The exponential dependence of elutriation rates on superficial air velocity can be expressed mathematically as

$$\dot{E} = ke^{\alpha V_s}. \qquad [1]$$

The parameter α is approximately constant for a given bed height and is not a function of the diffuser angle. This conclusion is based on the fact that the three sets of data in figure 1 exhibit approximately the same slope. In other words, linear fits to the three data sets would be almost parallel to one another. The parameter k, on the other hand, is a strong function of the diffuser opening angle and accounts for the shifts in the three data sets.

Since the gas-velocity profiles are approximately uniform, the gas velocity at the diffuser exit ought to vary inversely with the diffuser exit area. The elutriation rate would also be expected to have an inverse functional dependence on exit area of the diffuser. Mutually parallel fits to the three data sets were made, using the straight section as the base case. These fits, implicitly, yield the same value (~0.1 s/cm) for α in [1]. The corresponding values for k were 0.102, 0.048 and 0.031 g/min/cm^2 for the straight section and 20° and 40° diffusers, respectively. The diffuser expansion ratio A_E values are 1, 2.1 and 3.74, respectively. The product $k \cdot A_E$ is then seen to be almost constant. Put another way, the elutriation rate for a given bed height and air velocity scales inversely as the diffuser expansion ratio. This is in line with physical intuition and the findings of Kale & Eaton (1984a).

5. CONCLUSIONS AND RECOMMENDATIONS

On the basis of the discussion presented above, the major findings can be summarized as follows:

1. The time-averaged gas-velocity profile in the freeboard region is very uniform for small diffuser opening angles (<20°). In general, this conclusion will not hold if the bubble bursts are distributed nonuniformly across the bed surface.
2. Diffusers atop bubbling fluidized beds do not separate for opening angles as large as 60°, and this behavior is attributed to the effects of suspended particles in the diffuser flow. An order-of-magnitude analysis of the pressures involved supported this finding. Reduced velocities in the diffuser resulting from deceleration of the flow are responsible for a monotonic decrease in elutriation rate with increasing diffuser opening angles for small beds.

REFERENCES

ADAMS, E. W., EATON, J. K. & JOHNSTON, J. P. 1984 An examination of velocity bias in a highly turbulent separated and reattaching flow. *Proc. 2nd Int'l. Symposium on Applications of Laser Anemometry to Fluid Mechanics.*

CUTLER, A. D. & JOHNSTON, J. P. 1981 The effects of inlet conditions on the performance of straight-walled diffusers at low subsonic Mach numbers—a review. Report PD-26, Mechanical Engineering Department, Stanford University, Stanford, CA.

FOX, R. W. & KLINE, S. J. 1962 Flow regime data and design methods for curved subsonic diffusers. *Trans. ASME J. Basic Engng* **84,** 303–312.

HOFFMANN, J. A. 1981 Effects of free-stream turbulence on diffuser performance. *J. Fluids Engng* **103,** 385–390.

JAYARAMAN, R. 1982 An experimental study of the dynamics of an unsteady boundary layer. Ph.D. thesis, Stanford University, Stanford, CA.

KALE, S. R. & EATON, J. K. 1984a An experimental investigation of the effects of diffusers on elutriation rates from fluidized beds, in *Gas-Solid Flows* (Edited by Jurewicz, J. T.), ASME Vol. FED 10, New York, pp. 107–114.

KALE, S. R. & EATON, J. K. 1984b An experimental investigation of gas-particle flows through diffusers in the freeboard region of fluidized beds. Report MD-45, Mechanical Engineering Department, Stanford University, Stanford, CA.

KLINE, S. J. & MCCLINTOCK, F. A. 1953 Describing uncertainties in single-sample experiments. *Mech. Engng* January, 3–8.

LEVY, Y. & LOCKWOOD, F. C. 1983 Laser-Doppler measurements of flow in freeboard of a fluidized bed. *AIChE J.* **29,** 889–895.

MCLAUGHLIN, D. K. & TIEDERMAN, W. G. 1973 Biasing correction for individual realization of laser anemometer measurements in turbulent flows. *Phys. Fluids* **16,** 2082–2088.

STEVENSON, W. H. & THOMPSON, H. D. 1982 Direct measurement of laser-velocimeter bias errors in a turbulent flow. *AIAA J.* **20,** 1720–1723.